JACS
JOURNAL OF THE AMERICAN CHEMICAL SOCIETY
Communication
pubs.acs.org/JACS

New Crystal Structure: Synthesis and Characterization of Hexagonal Wurtzite MnO

Ki Min Nam,[†] Yong-Il Kim,[‡] Younghun Jo,[€] Seung Mi Lee,[‡] Bog G. Kim,[§] Ran Choi,[†] Sang-Il Choi,[†] Hyunjoon Song,[†] and Joon T. Park*[,†]

[†]Department of Chemistry, Korea Advanced Institute of Science and Technology (KAIST), Daejeon 305-701, Korea
[‡]Korea Research Institute of Standards and Science (KRISS), Daejeon 305-340, Korea
[€]Division of Materials Science, Korea Basic Science Institute (KBSI), Daejeon 305-333, Korea
[§]Department of Physics, Pusan National University, Pusan 609-735, Korea

Supporting Information

ABSTRACT: Most transition metal oxides have a cubic rocksalt crystal structure, but ZnO and CoO are the only stable transition metal oxides known to possess a hexagonal structure. Unprecedented hexagonal wurtzite MnO has been prepared by thermal decomposition of $Mn(acac)_2$ on a carbon template. Structural characterization has been carried out by TEM, SAED, and a Rietveld analysis using XRD. The experimental and theoretical magnetic results indicate magnetic ordering of the hexagonal wurtzite MnO. Density functional calculations have been performed in order to understand the electronic and piezoelectric properties of the newly synthesized hexagonal wurtzite MnO.

Transition metal oxides are an important group of materials, because they form a wide variety of structures, display many interesting properties, and have numerous applications.[1−4] Most transition metal oxides have a cubic rocksalt crystal structure,[5] but ZnO and CoO are the only stable transition metal oxides known to possess a hexagonal structure.[6,7] Since hexagonal CoO was observed in 1962,[7] a hexagonal metal oxide structure has not been discovered for five decades. Manganese oxide (MnO) is also known to have a cubic rocksalt crystal structure[8] and has attracted strong interest for its applications as catalysts, lithium-ion battery materials, and contrast-enhancement agents for magnetic resonance imaging (MRI).[9−12] The synthesis of hexagonal wurtzite MnO is unprecedented thus far. Magnetically ordered Mn^{2+} with a hexagonal wurtzite structure suggests the possibility of coupling magnetism and electric polarization, which would offer an extra degree of freedom in the design of conventional sensors, actuators, and energy storage devices.[13] Theoretical study of hypothetical hexagonal wurtzite MnO has suggested a large piezoelectric response with typical magnetic properties,[14] and its synthesis would have a major impact on further research in this field.

Herein, we report synthesis and characterization of hexagonal wurtzite MnO on a carbon template. In a typical synthesis, a carbon template for the synthesis of hexagonal wurtzite MnO was prepared from glucose under hydrothermal conditions at 160 °C, which is higher than the normal glycosidation temperature, leading to aromatization and carbonization.[15,16] The carbon template has a spherical morphology with a diameter in a range of 500 ± 50 nm (Figure S1 in the Supporting Information). A light brown slurry of $Mn(acac)_2$ (acac = acetylacetonate) in benzylamine with the carbon template was quickly heated to 180 °C under an Ar atmosphere. After being refluxed for 3 h, the reaction mixture was cooled to room temperature, producing hexagonal wurtzite MnO.

To obtain a reliable structural description of this new material, a Rietveld analysis using X-ray powder diffraction data was carried out. The single line fitting technique of the total pattern analysis solution program was used to extract the contribution of the crystalline phase from the diffraction pattern. Preliminary indexing of the diffraction pattern was performed using the pattern decomposition method, and the pattern was finally indexed by the space group assigned as $P6_3mc$ (No. 186, hexagonal wurtzite phase). A subsequent Le Bail profile fit was performed to extract the diffraction intensities and to refine the unit-cell parameters. The extracted intensities were used in the direct method (EXPO2009)[17] for the structure determination. The model determined using the direct method was refined by the Rietveld method (GSAS).[18] Figure 1 shows the Rietveld refinement patterns of hexagonal wurtzite MnO using the X-ray powder diffraction data (the final refined parameters are presented in Supporting Information Table S1). The interatomic distances of hexagonal wurtzite MnO have a short axial bond of 1.963(7) Å and three longer equatorial bonds of 2.0789(24) Å with a ratio of 0.944. The bonding angles of O−Mn−O in a tetrahedral coordination by oxygens are 110.55(17)° and 108.38(17)°, respectively (Table S2).

A transmission electron microscopy (TEM) image of the as-prepared hexagonal wurtzite MnO is presented in Figure 2a. The high resolution TEM (HRTEM) image in Figure 2b reveals that the observed lattice spacing corresponding to the (100) lattice plane is estimated to be 2.93 Å. The strong ring patterns from the selected area electron diffraction (SAED) can be indexed to the hexagonal wurtzite structure (Figure S2), which is consistent with the X-ray analysis provided in Figure 1.

Received: March 12, 2012
Published: May 7, 2012

dx.doi.org/10.1021/ja302440y | J. Am. Chem. Soc. 2012, 134, 8392−8395

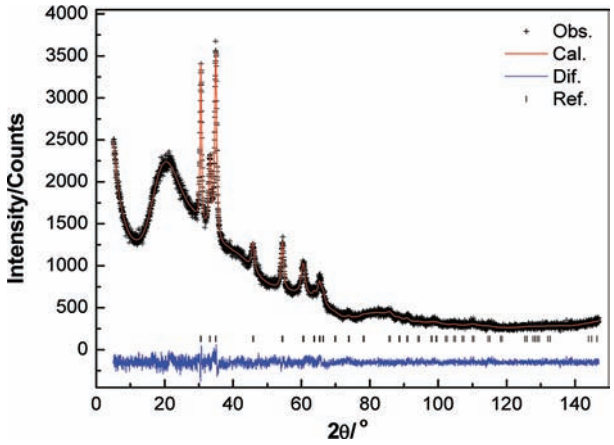

Figure 1. Rietveld refinement patterns of hexagonal wurtzite MnO using X-ray powder diffraction data. Plus marks (+) represent the observed intensities, and the red solid line is calculated result. The difference plot (blue) is shown at the bottom. Tick marks above the difference plot indicate the reflection positions, which are identified by Rietveld analysis. The hexagonal wurtzite parameters are as follows: space group $P6_3mc$ (No. 186) $a = b = 3.3718(2)$ Å, $c = 5.3854(7)$ Å. Mn at (1/3, 2/3, 0.0110) and O (1/3, 2/3, 0. 3755).

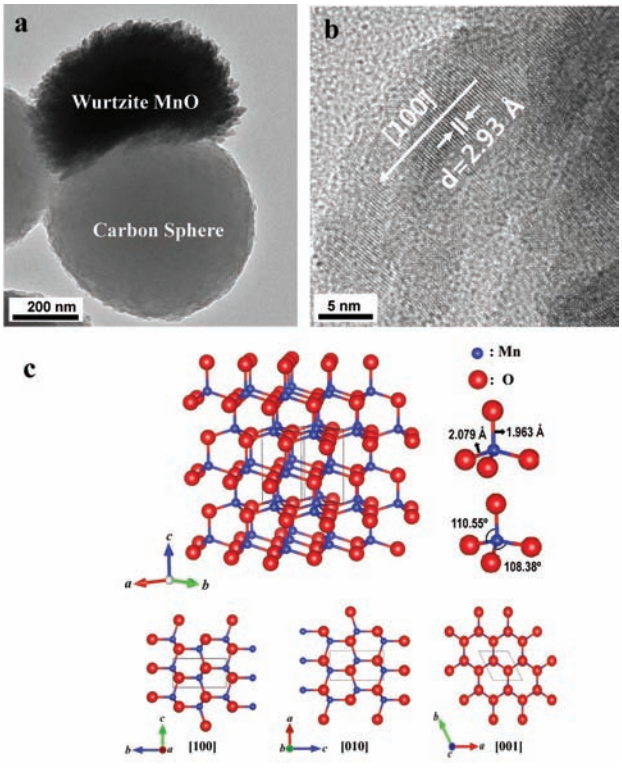

Figure 2. Micrographs of hexagonal wurtzite MnO. (a) Bright-field TEM image of hexagonal wurtzite MnO on the carbon sphere template; (b) HRTEM image of hexagonal wurtzite MnO; (c) crystal structure of hexagonal wurtzite MnO: crystal structure of MnO is projected along *a*-, *b*-, and *c*-axis, respectively.

Energy-disperse X-ray (EDX) spectrometry yielded an average atomic ratio of 48.7:51.3 (Mn/O) within an acceptable range of experimental error, indicative of the 1:1 atomic composition of hexagonal wurtzite MnO (Figure S3). The confirmed crystal structure of hexagonal wurtzite MnO is presented in Figure 2c. The hexagonal wurtzite structure of MnO can be described as a number of alternating planes composed of tetrahedrally coordinated Mn^{2+} and O^{2-} ions, stacked along the *c*-axis.

The magnetic properties of hexagonal wurtzite MnO were examined using a super conducting interference device (SQUID) magnetometer. Temperature dependence of the magnetic moment was investigated with zero-field-cooled and field-cooled schemes at 100 Oe as shown in Figure 3a. The

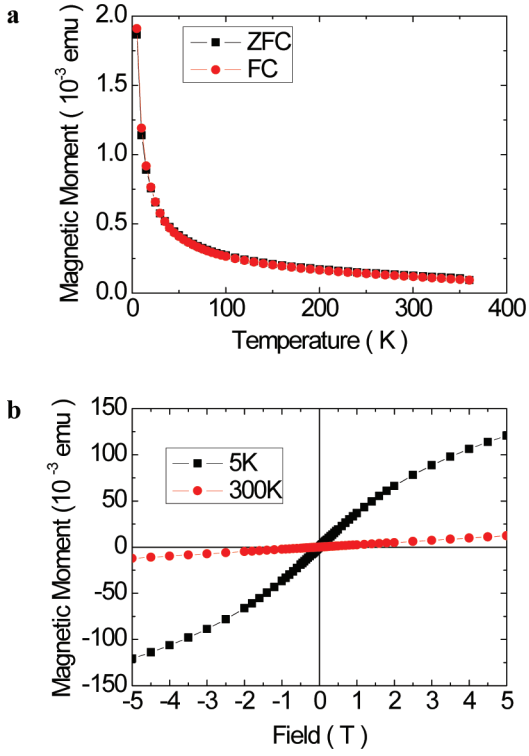

Figure 3. Magnetic susceptibility for hexagonal wurtzite MnO. (a) Zero-field-cooled (ZFC, black square) and field-cooled (FC, red circle) curves measured at 100 Oe; (b) magnetic-field dependence of magnetization measured at 5 K (black square) and 300 K (red circle).

magnetic moment of the hexagonal wurtzite MnO samples gradually increased with a decrease in the temperature and did not exhibit any magnetic transition down to 2 K. Figure 3b displays the magnetization (M) of the sample as a function of the magnetic field (H), acquired at two representative temperatures of 5 and 300 K. No hysteresis at either 5 or 300 K was observed; this indicates that the magnetic state in the temperature range does not change, which is consistent with the results for the temperature dependence of magnetization. The experimental results reveal paramagnetic behavior of hexagonal wurtzite MnO, and we were not able to identify an antiferromagnetic (AFM) transition, from either the temperature dependent or the field dependent mangnetization experiments, likely due to the nanosize samples of MnO. The energy differences in different magnetic orderings become extremely small when the sample size is nanoscale; this is related to the strong demagnetization effect due to the large surface area.[19,20]

To identify the magnetic structure of as-synthesized hexagonal wurtzite MnO, density functional calculations were carried out. Because the on-site Coulomb interactions play an important role in determining the magnetic and electronic properties of the MnO system, the GGA + U methods ($U_{eff} = 6$ eV) was employed. Details of the ab initio calculation are

dx.doi.org/10.1021/ja302440y | J. Am. Chem. Soc. 2012, 134, 8392−8395

described in the method section of Supporting Information. The energetics of the rocksalt and wurtzite structures with several antiferromagnetic and ferromagnetic (FM) orderings have been intensively investigated.[14,21] Our calculations using the structural parameters of hexagonal wurtzite MnO confirm that the AFM ordering is more stable than the FM ordering for hexagonal wurtzite structures. The lattice constants were optimized as a (= b) = 3.5194(3) Å, and c = 5.3794(5) Å after relaxation, using the structural parameters of hexagonal wurtzite MnO according to X-ray diffraction measurements ($P6_3mc$, No. 186 from Table S1). The lattice constants and magnetic moments of the Mn atom were calculated by the GGA + U methods for the hexagonal wurtzite structure with different magnetic configurations (Table S3). The most stable structure was calculated to have AFM ordering[21] for the hexagonal wurtzite MnO.

For Mn-doped ZnO, a potential candidate for dilute magnetic semiconducting (DMS) materials, it is anticipated that the substitution of Zn with Mn ($Zn_{1-x}Mn_xO$) would change the magnetic properties of ZnO from diamagnetism to ferromagnetism,[22,23] because Mn^{2+} in a tetrahedral oxygen environment is known to prefer ferromagnetic ordering. Thus, an extreme case of hexagonal wurtzite MnO ($Zn_{1-x}Mn_xO$, x = 1) is expected to have ferromagnetism. Our experimental and theoretical results of magnetism, however, indicate antiferromagnetism for hexagonal wurtzite MnO.

The electronic structure of hexagonal wurtzite MnO was also investigated. The total and projected densities of states are illustrated in Figure 4a. The projected density of states (PDOS) shows that the contributions both from the 3d electrons of the Mn atoms and the 2p electrons of the O atoms are dominant at the top of the valence band, while the 2p electrons of the O atoms contribute to the bottom of the conduction band. In the band structure of wurtzite MnO, the top of the valence band was nearly flat for specific k-points, and the bottom of the conduction band is at the Γ-point. However, the top of the valence band is at the L-point, and bottom of the conduction band is at the Γ-point in the cubic rocksalt structure. The band structures of cubic rocksalt and hexagonal wurtzite MnO with FM and AFM spin configuration are presented in Figure S6. The band gap energy of hexagonal MnO (AFM) was determined to be 1.58 eV while that of cubic MnO (AFM) was 1.99 eV.

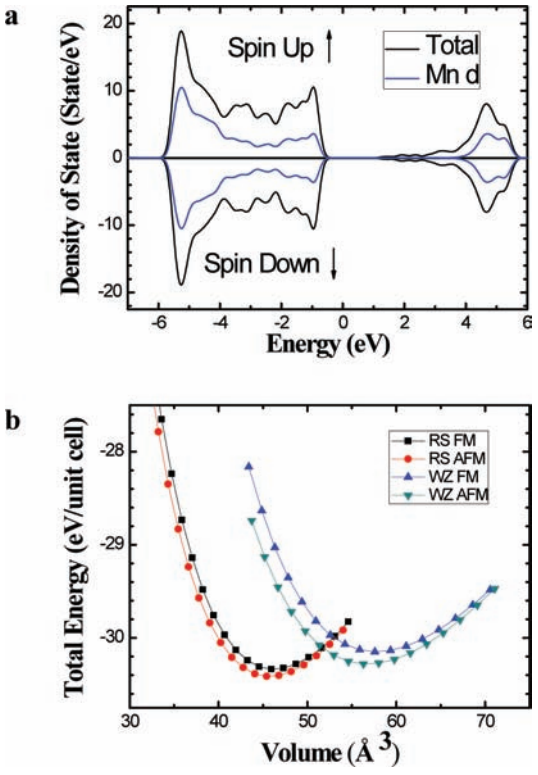

Figure 4. Theoretical results by density functional theory calculations on hexagonal wurtzite MnO. (a) Density of states (DOS) and projected density of states (PDOS) of the hexagonal wurtzite MnO; (b) total energy vs volume of ferromagnetic ordering (FM) and the antiferromagnetic orderings (AFM) for cubic rocksalt (RS) and hexagonal wurtzite MnO (WZ) structures.

The hexagonal wurtzite MnO has approximately 0.1 eV higher total energy compared to cubic rocksalt MnO, as shown in Figure 4b. The energy−volume analysis indicates that the hexagonal wurtzite structure of MnO is stabilized on a potential energy surface with a larger volume (negative pressure). If a large volume (extreme negative pressure) is applied to the cubic rocksalt structure, each Mn atom has six octahedral neighbor oxygens, and Mn atoms move in the z-direction and bond with four neighbor oxygen atoms instead of weakening six oxygen bonds equally. The carbon template has surface oxygen-functional groups,[16] which are hydrophilic and may induce the formation of hexagonal wurtzite MnO. Furthermore, the carbon and oxygen functional groups would significantly reduce the formation energy of a large volume structure, that is, a hexagonal wurtzite structure.[24] From charge and bonding analyses of the ab initio calculations, the chemical bonding effect seems to be the main driving force to form hexagonal wurtzite MnO on the carbon template. Other templates such as graphite, graphene, fullerene, and silica were used as templates, but instead of the hexagonal wurtzite phase, only a cubic rocksalt structure was yielded.

Piezoelectric generators can harvest electrical energy from the environment by converting mechanical energy into electricity.[25] The hexagonal wurtzite structure does not have a center of inversion symmetry,[26] and thus, a piezoelectric response is expected in hexagonal wurtzite MnO. Our ab initio calculation also confirms a double-well like energy surface as a function of the relative oxygen position in the hexagonal wurtzite MnO as shown in Figure S7, similar to ZnO. The amount of polar instability, which is closely related to the piezoelectric properties of hexagonal wurtzite MnO, is too high to be overcome by electric field. The piezoelectric constant e_{33} is calculated as 0.9973 (C/m^2). This value is comparable with that of ZnO (0.76−1.18 C/m^2),[27] which is the highest piezoelectric tensor among tetrahedrally bonded semiconductors.

In summary, we prepared new crystal structure on a carbon sphere template. This unprecedented MnO structure was identified by a Rietveld analysis using X-ray powder diffraction. The experimental and theoretical results indicate magnetic ordering of the hexagonal wurtzite MnO, which may help to understand the magnetism of Mn^{2+} in various oxygen environments. Density functional calculations provide the band gap energy (1.58 eV), and an energy−volume analysis indicates that the hexagonal wurtzite MnO is stabilized on a potential energy surface with a large volume. The hexagonal wurtzite MnO has a large piezoelectric constant based on ab initio calculation.

■ ASSOCIATED CONTENT

Supporting Information

Details of synthetic and computation procedures; XRD pattern, X-ray Rietveld analysis, and EDX results of hexagonal wurtzite MnO. Crystallographic information file (CIF) is available for the hexagonal wurtzite MnO. This material is available free of charge via the Internet at http://pubs.acs.org.

■ AUTHOR INFORMATION

Corresponding Author

joontpark@kaist.ac.kr

Notes

The authors declare no competing financial interest.

■ ACKNOWLEDGMENTS

This work was supported by the National Research Foundation (NRF) funded by the Korean Government (SRC Program: 20120000648), NSF of Korea (KRF-2011-0006055 and KRF-2012-0000964) and the New & Renewable Energy Technology Development Program (KETEP-20113020010050). Computational resources have been provided by KISTI Supercomputing Center (Project No. KSC-2011-C1-20). This work was also supported by NRF (No. 2011-0027908) of the MEST. We thank the staff of KBSI and KAIST for their assistance with the TEM analyses.

■ REFERENCES

(1) Poizot, P.; Laruelle, S.; Grugeon, S.; Dupont, L.; Tarascon, J.-M. *Nature* **2000**, *407*, 496.
(2) Seo, W. S.; Jo, H. H.; Lee, K.; Park, J. T. *Adv. Mater.* **2003**, *15*, 795.
(3) Wang, X.; Song, J.; Liu, J.; Wang, Z. L. *Science* **2007**, *316*, 102.
(4) Xie, X.; Li, Y.; Liu, Z.-Q.; Haruta, M.; Shen, W. *Nature* **2009**, *458*, 746.
(5) Roth, W. L. *Phys. Rev.* **1958**, *110*, 1333.
(6) Wang, Z. L. *Mater. Sci. Eng., R* **2009**, *64*, 33.
(7) Redman, M. J.; Steward, E. G. *Nature* **1962**, *193*, 867.
(8) Shaked, H.; Faber, J., Jr.; Hitterman, R. L. *J. Phys. Chem. B* **1988**, *38*, 11901.
(9) Seo, W. S.; Jo, H. H.; Lee, K.; Kim, B.; Oh, S. J.; Park, J. T. *Angew. Chem., Int. Ed.* **2004**, *43*, 1115.
(10) Sangaraju, S.; Gedanken, A. *J. Phys. Chem. B* **2006**, *110*, 24486.
(11) Na, H. B.; Lee, J. H.; An, K.; Park, Y. I.; Park, M.; Lee, I. S.; Nam, D.-N.; Kim, S. T.; Kim, S.-H.; Kim, S.-W.; Lim, K.-H.; Kim, K.-S.; Kim, S.-O.; Hyeon, T. *Angew. Chem., Int. Ed.* **2007**, *46*, 5397.
(12) Zhong, K.; Xia, X.; Zhang, B.; Li, H.; Wang, Z.; Chen, L. *J. Power Sources* **2010**, *195*, 3300.
(13) Ohno, H. *Science* **2000**, *281*, 951.
(14) Gopal, P.; Spaldin, N. A.; Waghmare, U. V. *Phys. Rev. B* **2004**, *70*, 205104.
(15) Hu, B.; Wang, K.; Wu, L.; Yu, S.-H.; Antonietti, M.; Titirici, M.-M. *Adv. Mater.* **2010**, *22*, 813.
(16) Sevilla, M.; Fuertes, A. B. *Chem.—Eur. J.* **2009**, *15*, 4195.
(17) Altomare, A.; Camalli, M.; Cuocci, C.; Giacovazzo, C.; Moliterni, A.; Rizzi., R. *J. Appl. Crystallogr.* **2009**, *42*, 1197.
(18) Larson, A. C.; Von Dreele, R. B. *Los Alamos Natl. Lab., [Rep.] LA (U. S.)* **1994**, 86.
(19) Zheng, X. G.; Xu, C. N.; Nishikubo, K.; Nishiyama, K.; Higemoto, W.; Moon, W. J.; Tanaka, E.; Otabe, E. S. *Phys. Rev. B* **2005**, *72*, 014464.
(20) Fisher, R.; Schrefl, T.; Kronmuller, H.; Fidler, J. *J. Magn. Magn. Mater.* **1996**, *153*, 35.
(21) Schron, A.; Rodl, C.; Bechstedt, F. *Phys. Rev. B* **2010**, *82*, 165109.
(22) Dietl, T.; Ohno, H.; Matsukura, F.; Cibert, J.; Ferrand, D. *Science* **2000**, *287*, 1019.
(23) Sharma, P.; Gupta, A.; Rao, K. V.; Owens, F. J.; Sharma, R.; Ahuja, R.; Guillen, J. M. O.; Johansson, B.; Gehring, G. A. *Nat. Mater.* **2003**, *2*, 673.
(24) Sakong, S.; Kratzer, P. *Semicond. Sci. Technol.* **2011**, *26*, 014038.
(25) Wang, Z.; Song, L. J. *Science* **2006**, *312*, 242.
(26) Hill, N. A.; Waghmare, U. *Phys. Rev. B* **2000**, *62*, 8802.
(27) Corso, A. D.; Poternak, M.; Resta, R.; Baldereschi, A. *Phys. Rev. B* **1994**, *50*, 10715.